

## Fermi-Dirac statistics and the nature of the compensating donors in boron-doped diamond layers

Johan F. Prins

*Schonland Research Centre for Nuclear Sciences, University of the Witwatersrand, Johannesburg 2050, South Africa*

(Received 28 July 1988; revised manuscript received 12 October 1988)

Fermi-Dirac statistics have been applied to semiconducting diamond layers doped with boron by means of ion implantation. Suitable limiting equations could be derived to describe the resistance-temperature behavior which relates to acceptor activation and also to hole creation in the valence band by means of compensating-donor neutralization. When applying these equations to the experimental data, it is found that the donor centers have a very large degeneracy weighting factor  $g_D$  and that this parameter depends on the annealing cycle used after ion implantation. This result can be explained by assuming that the donors consist of small aggregates of vacancies which constitute vacancy-lattice "crystallites." In this paper, we shall call these particular vacancy aggregates, which have a stable electronic structure, vacloids. The presence of vacloids may also be invoked to explain some of the optical properties previously observed in diamonds.

### I. INTRODUCTION

It was recently demonstrated that semiconducting layers with electrical and optical properties which correlate with those of natural  $p$ -type diamonds (type-IIb) could be manufactured in high-purity insulating (type-IIa) diamonds by means of ion implantation.<sup>1,2</sup> For this process, implantation needs to occur at a target temperature which is low enough to severely impede the diffusional motion of the implanted boron atoms as well as the vacancies and interstitials created in the collision cascades. Subsequent annealing then enhances the probability of boron-atom activation and interstitial-vacancy recombination owing to their high density and proximity to each other. The activation ratio  $R$  could be defined<sup>1</sup> as the fraction of the initial (as implanted) vacancy number density  $N_{v0}$  which recombined with interstitials during the annealing stage, given by

$$R = 1 - \frac{N_{v\text{res}}}{N_{v0}}, \quad (1)$$

where  $N_{v\text{res}}$  is the residual density of vacancies which did not recombine with interstitials.  $R$  only describes the "activation," or rather recombination, of vacancies with self-interstitials. However, it may be applied to the activation of the implanted boron atoms if it is assumed that a boron interstitial and a self-interstitial have an equal chance to jump into a vacancy.

An expression for  $N_{v\text{res}}$  can be derived if the probability  $P$  for vacancy-interstitial recombination during the annealing stage is known. When implanting diamond at a temperature where interstitials can diffuse but not the vacancies, a reasonable description of the process was obtained by assuming that the probability for recombination is given by<sup>3</sup>

$$P = \beta\omega \left[ \frac{N_v}{N} \right], \quad (2)$$

where  $N_v$  is the average vacancy density in the ion-damaged width  $\omega$ ,  $N$  is the density of atoms in a perfect diamond crystal, and  $\beta$  a temperature-dependent parameter. The doping process described above may require a more elaborate probability function than that given in Eq. (2). However, using this equation, an expression for  $N_{v\text{res}}$  could be derived<sup>1</sup> which seems to describe the doping process, at least in principle, when annealing occurs at a temperature where interstitial diffusion dominates, i.e.,

$$N_{v\text{res}} = \begin{cases} N_{v0} \exp \left[ -\beta\omega \frac{N_{v0}}{N} \right] & \text{for } \beta\omega(N_{v0}/N) \leq 1, \\ N(\beta\omega e)^{-1} & \text{for } \beta\omega(N_{v0}/N) > 1. \end{cases} \quad (3)$$

The initial experiments, designed to test the ideas outlined above, were performed using a two-stage annealing cycle.<sup>1</sup> After implantation at liquid-nitrogen temperature, the diamonds were heated directly to 500 °C by dropping them onto a preheated platform. It is believed that at this temperature all the interstitials can diffuse but not the vacancies.<sup>1,3</sup> This was followed by a further anneal at 1200 °C in order to reduce the residual vacancies. These implanted layers displayed impurity conduction and, under suitable implantation conditions, resistance-temperature behavior which correlated with the activation of holes from boron acceptors to the valence band at the expected activation energy of  $\sim 0.37$  eV (Ref. 4). At high temperatures, an even larger activation energy ( $\sim 0.8$  eV) could be measured for the electrical conduction, and this was associated with electrons being activated to charged deep-level donors, in this way creating

more holes in the valence band. From the magnitude of the latter effect it was evident that the acceptor compensation ratio must be very large.

The presence of the deep donor centers also correlates with increased optical absorption towards shorter wavelengths.<sup>1</sup> Similar absorption features are usually present in natural type-IIa diamonds,<sup>5</sup> giving them a brownish hue. Clark, Ditchburn, and Dyer<sup>6</sup> thought that this absorption could be caused by small graphitic regions in the diamond. Alternatively, the suggestion was made that these small regions may not be graphitic but only contain a high density of vacancies<sup>7</sup> caused by the clustering of these defects.

The latter idea ties in very well with the nature of the donors expected to remain after doping diamond by means of ion implantation. As outlined above, the mechanism by which doping is achieved causes the residual radiation damage after annealing to be in the form of vacancies or more complex defects caused by their interaction.

In this study, Fermi-Dirac statistics combined with the doping theory developed previously<sup>1</sup> are applied to the semiconducting diamond layers which were obtained by means of ion implantation.<sup>1,2</sup> More information about the electrical and probable physical properties of the resulting donor centers is obtained, as well as a deeper insight into the validity of Eqs. (1)–(3).

## II. THEORETICAL CONSIDERATIONS

As already mentioned, the semiconducting diamond layers obtained by boron-ion implantation show the presence of  $N_A$  boron acceptors at an activation energy of  $E_A = 0.37$  eV, which are heavily compensated by  $N_D$  deep-level donors lying at an energy  $E_D$  above the valence band.<sup>1,2</sup> At a temperature  $T$ , there will be  $p$  holes in the valence band, and  $N_A^-$  and  $N_D^+$  ionized acceptors and donors, respectively, so that for charge neutrality

$$N_D^+ + p = N_A^- . \quad (4)$$

From the standard equilibrium statistics applicable to an electron gas,<sup>8</sup> expressions for  $N_A^-$  and  $N_D^+$  follow as

$$N_A^- = \frac{N_A}{1 + g_A \exp \left[ \frac{E_A - E_F}{kT} \right]} \quad (5)$$

and

$$N_D^+ = \frac{N_D}{1 + g_D \exp \left[ \frac{E_F - E_D}{kT} \right]} , \quad (6)$$

where  $E_F$  is the Fermi energy,  $k$  is Boltzmann's constant, and  $g_A$  and  $g_D$  are the degeneracy weighting factors for the acceptors and donors, respectively. For the boron acceptor in diamond, the value of  $g_A$  is usually assumed to be 2.<sup>4</sup> If the energy at the top of the valence band is taken as zero, the standard expression for a nondegenerate distribution of holes in the valence band follows as

$$p = N_V \exp \left[ -\frac{E_F}{kT} \right] ,$$

where

$$N_V = 2 \left[ \frac{2\pi m^* kT}{h^2} \right]^{3/2} . \quad (7)$$

As usual,  $h$  is Planck's constant and  $m^*$  an averaged effective mass for the holes.<sup>8</sup> Combining Eqs. (4)–(7), and making the following substitutions,

$$\phi_A = \exp \left[ -\frac{E_A}{kT} \right] , \quad (8)$$

$$\phi_D = \exp \left[ -\frac{E_D}{kT} \right] , \quad (9)$$

and

$$Z = \frac{p}{N_A} , \quad (10)$$

lead to a standard cubic equation

$$Z^3 + AZ^2 - BZ - C = 0 , \quad (11)$$

where

$$A = N_A^{-1} [N_D + g_A^{-1} N_V (\phi_A + g_A g_D \phi_D)] , \quad (12)$$

$$B = g_A^{-1} N_A^{-2} N_V \phi_A [(N_A - N_D) - g_D N_V \phi_D] , \quad (13)$$

$$C = g_A^{-1} g_D N_A^{-2} N_V^2 \phi_A \phi_D . \quad (14)$$

Because  $E_D$  is larger than  $E_A$  (in this case  $E_D > E_A + 0.8$  eV), the exponential factor  $\phi_D$  is very small and the terms containing it can usually be neglected. When this is done, Eq. (11) leads to the standard expression for a compensated  $p$ -type semiconductor, which is normally applied to type-IIb diamonds.<sup>4</sup> However, for a highly doped semiconductor ( $N_A$  large) with a very high compensation ratio ( $N_D$  also large with  $N_A - N_D$  small by comparison) two different limiting forms of Eq. (11) become evident. This may be seen by writing down the general solution for this equation. In the temperature range of interest,  $p \ll N_A$ , allowing  $Z^3$  to be neglected. Equation (11) then becomes quadratic with the solution expressed as

$$Z = \left[ \left[ \frac{C}{A} \right]^2 + \left[ \frac{B}{2A} \right]^2 \right]^{1/2} + \left[ \frac{B}{2A} \right] . \quad (15)$$

At low temperatures  $\phi_D$  is very small and for  $g_D N_V \phi_D \ll N_A - N_D$  the terms containing  $\phi_D$  in Eqs. (12)–(14) may be neglected. In this case  $C \approx 0$  in Eq. (15) and the solution for the density of holes  $p_1$  in the valence band becomes

$$p_1 \approx N_A \left[ \frac{B}{A} \right] = g_A^{-1} N_V \left[ \frac{N_A}{N_D} - 1 \right] \exp \left[ -\frac{E_A}{kT} \right] . \quad (16)$$

As the temperature increases,  $\phi_D$  and  $N_V$  also increase, causing the coefficient  $C$  to become non-negligible. In

concert, the value of  $B$  decreases, finally making the above approximation invalid. When  $B$  becomes negligible and  $C$  dominates, the hole density  $p_2$  follows approximately as

$$p_2 \approx N_A \left[ \frac{B}{2A} + \left( \frac{C}{A} \right)^{1/2} \right] \\ = \frac{1}{2} p_1 + N_V \left[ \frac{g_D N_A}{g_A N_D} \right]^{1/2} \exp \left[ -\frac{E_A + E_D}{2kT} \right]. \quad (17)$$

### III. APPLICATION TO EXPERIMENTAL RESULTS

Resistance-temperature curves which display low- and high-temperature limiting forms commensurate with Eqs. (16) and (17) are shown in Fig. 1. These curves were selected from previously published results.<sup>1,2</sup> According to the implantation scheme used to obtain these data, different ratios of boron to carbon ions were implanted to ensure, in each case, that the same average initial density of vacancies  $N_{v0}$  distributed in the same manner over the ion-damaged width  $\omega$  was obtained, even though the number of boron ions implanted varied. In this way, different numbers of boron atoms could be activated during annealing while ending up with the same density of unrecombined vacancies for the same annealing cycle

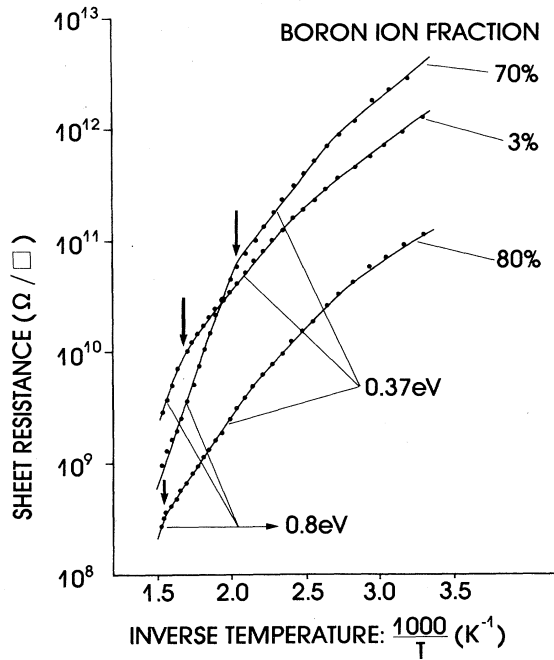


FIG. 1. Resistance-temperature curves of three diamond layers which were doped by means of ion implantation using different boron-ion fractions. The 70% and 80% curves were obtained by a two-stage annealing process, first annealing at 500°C and then 1200°C (Ref. 1). More efficient annealing was obtained for the 3% curve by fast and direct heating to  $\sim 1200^\circ\text{C}$  (Ref. 2).

TABLE I. Energy and ion-dose distribution used for a 100% boron-ion implantation. The number of vacancies created per impinging ion ( $\alpha$ ) as predicted by TRIM86 (Ref. 9), for a displacement energy of 55 eV, is also displayed.

Energy (keV)	Ion dose ( $\text{cm}^{-2}$ )	Vacancies per ion $\alpha^a$
120	$2.8 \times 10^{15}$	89
70	$2.0 \times 10^{15}$	75
45	$1.0 \times 10^{15}$	59

<sup>a</sup>Average number of vacancies per ion,  $\alpha = 79$ .

used. If a boron-ion dose of  $S \text{ cm}^{-2}$  is needed to cause the  $\omega N_{v0}$  vacancies, then

$$N_{v0} \approx \frac{\alpha S}{\omega}, \quad (18)$$

where  $\alpha$  is the average number of vacancies created per impinging ion. For an  $X\%$  boron-ion fraction implanted,  $(100-X)\%$  of the vacancies was first introduced using an equivalent carbon-ion dose, followed by  $X\%$  of the boron dose  $S$ .<sup>1,2</sup> Before annealing, the average density of implanted boron atoms would thus be  $N_B(X)$ , where

$$N_B(X) = \frac{XS}{100\omega}. \quad (19)$$

The boron dose,  $S = 5.8 \times 10^{15} \text{ cm}^{-2}$ , was spread over the three energies shown in Table I, which also shows the average number of vacancies  $\alpha$  per ion according to TRIM86 (Ref. 9), assuming a displacement energy of 55 eV.<sup>3</sup>

Figure 1 shows the results obtained for 70% and 80% boron-ion fractions subjected to a two-stage anneal (first heating to 500°C and then finally annealing at 1200°C).<sup>1</sup> and a 3% boron-ion fraction which was directly heated to  $\approx 1200^\circ\text{C}$ .<sup>2</sup> Obviously the activation ratio  $R$  was much larger in the latter case. At low temperatures, each curve displays conduction at smaller activation energies. This is probably a result of the high compensation ratio, which could cause hopping conduction between charged and neutral acceptors.<sup>1</sup> As the temperature increases, a region is reached with an activation energy of 0.37 eV which may, accordingly, be approximated by Eq. (16). At high temperature, another inflexion point is reached where the slope changes to a larger value of  $\sim 0.8 \text{ eV}$ . If Eq. (17) is now valid, it would mean that  $E_D + E_A \approx 1.6 \text{ eV}$ , and thus  $E_D \approx 1.23 \text{ eV}$ . From Eq. (15) the latter inflexion point occurs when  $(B/A)^2 = 4C/A$ , which with the aid of Eqs. (12)–(14), renders

$$g_A g_D \approx \frac{1}{4} \left[ \frac{N_A}{N_D} \right]^{-1} \left[ \frac{N_A}{N_D} - 1 \right]^2 \exp \left[ \frac{E_D - E_A}{kT} \right]. \quad (20)$$

Basically, this equation contains only two unknowns, i.e.,  $g_A g_D$  and  $N_A/N_D$ . A boron activation ratio  $R_A$ , such that

$$N_A = R_A N_B(X), \quad (21)$$

in conjunction with Eqs. (18) and (19), gives

$$\frac{N_A}{N_D} = Xy, \quad (22)$$

where

$$y = \left[ \frac{R_A N_{v0}}{100\alpha N_D} \right]. \quad (23)$$

When Eq. (22) is substituted into Eq. (20), the latter equation is determined by the unknown factors  $g_A g_D$  and  $y$  (because  $X$  is known).

For the 70% and 80% curves in Fig. 1, which went through the same annealing sequence, the unknown factors  $g_A g_D$  and  $y$  should be the same. Thus, applying Eq. (20) to these curves at their inflexion temperatures (shown by the arrows), assuming  $E_A = 0.37$  eV and  $E_D = 1.23$  eV, renders the following values for  $y$  and  $g_A g_D$ :

$$y = 1.45 \times 10^{-2},$$

and

$$g_A g_D = 3.85 \times 10^4.$$

Setting  $g_A = 2$ , as is normally done for diamond, still leaves a value of  $1.9 \times 10^4$  for the donor-degeneracy weighting factor  $g_D$ , which is enormous. Even in the unlikely event that the slope at high temperatures was inaccurately determined by an amount of 0.1 eV, a recalculation of the results using a value of 0.7 eV (for which  $E_D = 1.03$  eV) still gives a very large value for  $g_D$ , i.e.,  $g_D = 1.16 \times 10^3$ .

The 3% curve (Fig. 1) was obtained using a different annealing cycle, which obviously changed  $R_A$ ,  $N_D$ , and thus the value of  $y$ . An estimate of this new value of  $y = y'$  can be determined from Eq. (20) if it is assumed that the donor centers active in the latter case have the same value for  $g_D$  as previously determined. The solutions obtained at the inflexion temperatures are summarized in Table II.

Even though the resistances shown in Fig. 1 were not obtained using a four-point probe, and the carrier mobilities are not known, it is an interesting exercise to compare the parameters displayed in Table II with the equivalent ones found using the actual resistances measured, remembering that the resistance should be inversely proportional to the number of holes in the valence band, as described by either Eq. (16) or (17).

At a temperature of 200°C [(1000 K)/ $T = 2.12$ ], the 0.37 eV sections for the 80% and 70% curves overlap,

and the ratio of the sheet resistance  $R_S(70\%)$  for the 70% curve to the resistance  $R_S(80\%)$  for the 80% curve comes to  $10^{1.3}$ . The corresponding number of holes  $p(80\%)$  and  $p(70\%)$  can be calculated in terms of  $y$  using Eqs. (16) and (22). Assuming that the mobilities for the holes in the two cases, are the same, the following relationship should be valid:

$$10^{1.3} = \frac{R_S(70\%)}{R_S(80\%)} = \frac{p(80\%)}{p(70\%)} = \frac{80y - 1}{70y - 1}. \quad (24)$$

From this equation, the magnitude of  $y$  follows as  $y = 1.439 \times 10^{-2}$ , showing a remarkable correspondence (within 1%) to the value obtained in Table II. Taking the average of the two values, gives  $y = 1.444 \times 10^{-2} \pm 5 \times 10^{-5}$ . Similarly, for temperatures below 215 and above 156°C, the 3% and 70% segments with activation energies of 0.37 eV overlap, giving a resistance ratio of  $10^{0.22}$ . Again in this case

$$10^{0.22} = \frac{R_S(70\%)}{R_S(3\%)} = \frac{p(3\%)}{p(70\%)} = \frac{3y' - 1}{70y - 1}. \quad (25)$$

Thus, using the average value obtained for  $y$  above, one may calculate  $y'$  which results in  $y' = 3.393 \times 10^{-1} \pm 1.9 \times 10^{-3}$ , compared to  $y' = 3.6305 \times 10^{-1}$  obtained previously (see Table II). At first glance the correspondence looks fair, but Eq. (20) is very sensitive to small changes in the parameter  $y$ . For example, accepting the new value  $y = y' = 3.393 \times 10^{-1}$ , and recalculating  $g_A g_D$  for the 3% curve using this equation renders  $g_A g_D = 1.66 \times 10^3$ , which is an order of magnitude less than that obtained from the 70% and 80% curves (Table II). It may be reasoned that Eq. (25) should be altered by the ratio of the hole mobilities applicable to the 3% and 70% curves, respectively. However, to remove the discrepancy in this way would require the hole mobility to be less for the 3% curve (by a factor of  $\sim 4$ ). Physically, this is highly unlikely in view of the better activation achieved, which should have diminished the residual radiation damage compared to that of the 70% curve. The only alternative is to accept that  $g_D$  is in fact smaller for the 3% curve.

Further support for the latter conclusion is found when the ratios of the resistances measured for the 0.8 eV sections (Fig. 1) are compared with the hole ratios as calculated using Eq. (17) in conjunction with Eq. (22). As a suitable overlapping temperature at which to calculate the hole ratios for comparison with the corresponding resistance ratios, 360°C was selected. Using the value of  $y (= 1.444 \times 10^{-2} \pm 5 \times 10^{-5})$  described above, together

TABLE II. The values of the parameter  $y$  and the degeneracy-weighting factor  $g_D$  as determined from the 70% and 80% curves in Fig. 1. Assuming  $g_A g_D$  to be the same for the 3% curve, the corresponding factor  $y'$  was also calculated.

Boron-ion fraction used	80%	70%	3%
Inflexion temperature from Fig. 1 (°C)	360	215	320
$\exp[(E_D - E_A)/kT]$ at inflexion temperature	$7.05 \times 10^6$	$7.68 \times 10^8$	$2.11 \times 10^7$
$y$ [see Eq. (23)]	$1.449 \times 10^{-2}$	$1.449 \times 10^{-2}$	$y' = 3.631 \times 10^{-1}$
$g_A g_D$ (as determined from 70% and 80% curves)		$3.85 \times 10^4$	

with the value of  $y' = 3.631 \times 10^{-1}$  in Table II, where it was assumed that  $g_D$  is the same for each curve, the correspondence between the resistance and hole ratios is reasonable only when comparing the 70% and the 80% curves, but not when comparisons are made using the 3% curve (see columns 2 and 3 of Table III). However, when using the average value of  $y = 1.444 \times 10^{-2}$  together with  $y' = 3.393 \times 10^{-1} \pm 1.9 \times 10^{-3}$ , reasonable correspondence is found when taking ratios with the 3% curve (see columns 2 and 4 of Table III). This again indicates that  $g_D$  is the determining factor, and that this parameter is totally different for the 3% curve.

As a first approximation, it seems reasonable to assume that the hole mobilities are approximately the same for the three curves, which requires  $g_D \approx 1.93 \times 10^4$  for the 70% and 80% curves but a lower value  $g_D \approx 830$  for the 3% curve. Small differences, if any, between the hole mobilities are not unexpected for highly compensated semiconductors. In fact it is possible to determine the approximate magnitude of the average mobility  $\mu$ . By using the appropriate equation [either (16) or (17)], the number of holes at a chosen temperature may be calculated and compared to the corresponding resistivity measured. If it is assumed that the width of the layer is  $\omega \approx 0.2 \mu\text{m}$ ,<sup>1</sup> the mobility comes to  $\mu \approx 2.5 \text{ cm}^2 \text{ V}^{-1} \text{ s}^{-1}$ .

#### IV. DISCUSSION

The two limiting expressions in Eqs. (16) and (17) are plausible descriptions of the resistance-temperature behavior shown by the segments with slopes of 0.37 and 0.8 eV, respectively (see Fig. 1). However, when applying these expressions to the measured data, the degeneracy weighting factor  $g_D$  obtained for the donors is very large and inconsistent, in that it seems to be dependent on the annealing cycle employed. It is unlikely that this situation resulted from the approximations made when expressions (16) and (17) were derived and equated. In fact, if charged compensating donors are responsible for the creation of holes in the valence band at these temperatures subject to an activation energy of 0.8 eV, it can only happen for  $g_D$  large. This situation could logically relate to that of each donor being an aggregate of many vacan-

cies, as was proposed above.

Intuitively, one may reason that small stable regions of high vacancy density should form in a diamond when a supersaturated "soup" of vacancies "segregates" out during diffusion. When vacancies diffuse together, they lower the density of the material in that region. Owing to the metastability of diamond, a lowering in the material density will provide a strong driving force to form graphite. It is possible that once a certain critical vacancy density has been reached, the region containing these vacancies will prefer to become totally graphitic. If the material density in that volume is not yet that of graphite, a further volume expansion will be needed to effect the phase transformation. However, the region is surrounded by a very rigid diamond matrix which prevents this expansion and thus supplies the necessary pressure to stabilize the structure. In this way, the vacancy structure could be "immobilized." Newly arriving vacancies can now only add on to the surface of this region to enlarge it. The interface between this vacancy-rich region and the matrix should have a surface energy associated with it which may finally stabilize the size to which this defective volume can grow.

Alternatively, if the vacancies are considered as "atoms" diffusing together to form a "vacancy-type solid," or vacancy-carbon-atom "superlattice," it is conceivable that this small "crystal" may contain its electrons in a very narrow (because of its small size) energy band. Effectively, this will mean that the ground state of this donor-type defect may be considered as highly degenerate which can, in this way, account for the large values found for  $g_D$ . It is also conceivable that the average number of vacancies which aggregate to form such a defect will depend on the annealing cycle employed, which explains the variation observed in  $g_D$  when applying Eq. (17) directly to the different curves in Fig. 1. It is proposed that such "vacancy-lattice" regions should be termed "vacloids."

To obtain an estimate of the number of vacancies  $h$  which diffused together to form a vacloid, one may note that four covalent bonds are broken when a vacancy is created, which indicates that each vacancy may add eight units to the degeneracy weighting factor  $g_D$ . Using the

TABLE III. Comparison of the resistance ratios at 360°C for the different curves in Fig. 1 with the hole ratios calculated at this temperature from Eq. (17). In column 3 the hole ratios were calculated on the assumption that the degeneracy-weighting factor  $g_D$  is the same for all three curves. Column 4 shows the ratios obtained when using the corrected but different value of  $g_D$  for the 3% curve.

Curves compared	Resistance ratios	Hole ratios from Eq. (17) assuming $g_D$ to be the same, using $y = 1.444 \times 10^{-2} \pm 5 \times 10^{-5}$ and $y' = 3.631 \times 10^{-1}$	Hole ratios from Eq. (17) assuming $g_D$ to be different for the 3% curve, using $y = 1.444 \times 10^{-2}$ and $y' = 3.393 \times 10^{-1} \pm 1.9 \times 10^{-3}$
70% and 80%	$\frac{R_S(70\%)}{R_S(80\%)} = 10^{0.35} = 2.24$	$\frac{P(80\%)}{P(70\%)} = 2.5^{+1.12}_{-0.55}$	
3% and 70%	$\frac{R_S(3\%)}{R_S(70\%)} = 10^{0.55} = 3.55$	$\frac{P(70\%)}{P(3\%)} = 0.042^{+0.3}_{-0.036}$	$\frac{P(70\%)}{P(3\%)} = 2.52^{+1.19}_{-0.60}$
3% and 80%	$\frac{R_S(3\%)}{R_S(80\%)} = 10^{0.9} = 7.94$	$\frac{P(80\%)}{P(3\%)} = 1.27^{+0.04}_{-0.03}$	$\frac{P(80\%)}{P(3\%)} = 6.35^{+2.97}_{-1.53}$

values obtained for  $g_D$  in the preceding paragraph and dividing them by 8 renders an average of  $h = 2410$  vacancies per vacloid for the 70% and 80% curves, and  $h' = 104$  vacancies for the 3% curve. It is expected that the material density of a vacloid should be larger than that of graphite or else relaxation to a graphitic phase will occur. However, an order of magnitude value for the size of a vacloid may be obtained if it is assumed that the vacancies became stabilized to form this region at the material density of graphite. Assuming a spherical geometry, the diameters for the two sizes of vacloids come to  $\sim 42 \text{ \AA}$  (for the 70% and 80% curves) and  $\sim 15 \text{ \AA}$  (for the 3% curve). Dechanneling measurements by Derry *et al.*<sup>10</sup> on diamond which had been annealed after light ion damage, correlate with the presence of defects having diameters in the range 10–50  $\text{\AA}$ . Vandersande<sup>11</sup> studied the thermal conductivity of electron-irradiated diamonds and came to the conclusion that the point defects created by the electrons cluster during annealing at 1100 °C to form aggregates with an average diameter of  $\sim 55 \text{ \AA}$ . At low temperatures, after irradiation and before annealing, he observed larger aggregates ( $\sim 200 \text{ \AA}$ ) which could not have been formed by vacancy diffusion, if it is assumed that vacancies only become mobile well above 500 °C. He concluded that these large aggregates consisted of interstitials and reasoned accordingly that the 55  $\text{\AA}$  aggregates found after annealing are the same. In view of the doping theory developed<sup>1</sup> and the present results derived from it, it seems reasonable to propose that the latter aggregates were vacloids.

Pereira and Jorge<sup>12</sup> concluded from their optical studies on brown diamonds that the presence of sharp low-energy vibronic progressions in several of the luminescence bands analyzed may be due to a nearly localized vibrational mode, showing a weak coupling to resonant lattice phonons. Although they suggested that this mode was probably caused by impurity atoms, they did not rule out a softening of the force constant within a localized region as an explanation for their results. A vacloid, as proposed here, will be a region where a localized softening of the force constant between the atoms should occur. The correspondence between the optical absorption displayed by "brown" diamonds and the absorption resulting from the radiation damage remaining after electron irradiation or ion implantation, indicate that vacloids may already be present in natural diamonds.

More information about vacloids and the doping achieved would have been possible if it was known how  $N_D$  and  $N_{v0}$  related to each other. According to the interpretation of the initial doping experiments, the density of donor centers  $N_D$  which remains after annealing is

determined by the fate of the unrecombined vacancies of donor centers  $N_D$  which remains after annealing is determined by the fate of the unrecombined vacancies  $N_{vres}$ . During the annealing cycle, at which these vacancies can diffuse, some may escape from the ion-damaged layer, while the rest are assumed to be responsible for the formation of the above-mentioned donors. Thus, the smaller  $N_{vres}$  becomes, the lower the density of the donors  $N_D$  should be. According to Eq. (3) this would require a large  $N_{v0}$ ,  $\omega$ , and  $\beta$ , which in turn requires an optimization of the implantation parameters and the subsequent annealing cycle. If  $N_D$  is primarily a function of  $N_{vres}$ , Eq. (1) implies a simple relationship between  $N_D$ , the initial vacancy density  $N_{v0}$ , and the activation ratio  $R$ . For example, if it is assumed that all the residual vacancies  $N_{vres}$  aggregated to form vacloids, the average number of vacancies ( $h$ ) per vacloid will be

$$h = \frac{N_{vres}}{N_D} \quad (26)$$

A combination of Eqs. (1) and (26) then gives the needed relationship between  $N_D$  and  $N_{v0}$ , i.e.,

$$N_D = h^{-1} N_{v0} (1 - R) \quad (27)$$

Substituting this expression into Eq. (23) and using the values  $h = 2410$  and  $y = 1.444 \times 10^{-2}$  for the 70% and 80% curves, and  $h' = 104$  and  $y' = 3.3393 \times 10^{-1}$  for the 3% curve, allows some insight into the magnitudes for the activation ratios which were obtained. For  $\alpha = 79$  and  $R_A = R$  the activation ratio for the 70% and 80% curves is found to be  $R_1 = 0.05$  and that for the 3% curve  $R_2 = 0.96$ . The improvement could thus be 19 times and not  $\sim 7$  times, as was roughly deduced before.<sup>2</sup>

Using Eq. (3) together with Eqs. (1) and (18) allows the corresponding value of  $\beta$  to be calculated when  $R = R_1 = 0.05$ , and it is found to be  $\beta \sim 2 \mu\text{m}^{-1}$ . Although of the correct order of magnitude, it is a bit smaller than could have been expected from previous data. Measurements of the volume expansion and saturation of this expansion with ion dose when implanting a diamond above room temperature<sup>3</sup> led to the conclusion that  $\beta \sim 8 \mu\text{m}^{-1}$  at an implantation temperature (caused by beam heating) of about 100 °C. Various reasons may be advanced for this apparent discrepancy. For example,  $h$  may have been overestimated when assuming that each vacancy contributes only 8 units to  $g_D$ , or  $\alpha$  underestimated by assuming a displacement energy of 55 eV in the TRIM86 (Ref. 9) computer program. Furthermore, the value of  $\beta = 8 \mu\text{m}^{-1}$  (Ref. 3) was determined when annealing occurred during the implantation process. In

TABLE IV. Donor and acceptor densities calculated for the three different boron-doped diamond layers used in this study.

Boron-ion fraction (%)	Donors $N_D$ ( $\text{cm}^{-3}$ )	Acceptors $N_A$ ( $\text{cm}^{-3}$ )	Uncompensated acceptors $N_A - N_D$ ( $\text{cm}^{-3}$ )
3	$8.205 \times 10^{18}$	$8.352 \times 10^{18}$	$1.47 \times 10^{17}$
70	$1.004 \times 10^{19}$	$1.015 \times 10^{19}$	$1.10 \times 10^{17}$
80	$1.004 \times 10^{19}$	$1.160 \times 10^{19}$	$1.56 \times 10^{18}$

that case, the interstitial concentration remained low compared to the vacancy concentration. For the situation presently considered, the annealing stage initiates when the vacancies and interstitials have nearly equal concentrations. It is then possible that more interstitials can escape, which would mean a lower effective  $\beta$ . Alternatively, it could also mean that the probability function [Eq. (2)] needs to be adjusted which, in turn, will change Eq. (3). Even so, when applying the latter equation to the results obtained for rapid high-temperature annealing (3% curve), the value of  $\beta$  corresponding to  $R=R_2=0.96$  comes to  $\beta=355 \mu\text{m}^{-1}$ , indicating a very marked increase in interstitial-vacancy recombination.

If it is further assumed that the quantities  $R_1=0.05$  and  $R_2=0.96$  are indeed valid, then the average values for  $y$  and  $y'$  derived above can be used to obtain a measure of the number of acceptors  $N_A$  and donors  $N_D$  for each of the curves displayed in Fig. 1. Using again  $\omega=0.2 \mu\text{m}$  in conjunction with Eqs. (19)–(21) renders the values for  $N_A$ ,  $N_D$ , and  $N_A-N_D$  shown in Table IV. These numbers compare favorably to the values of  $N_A-N_D$  which were determined for natural semiconducting diamonds.<sup>4</sup> This is a gratifying result, especially in view of the approximations which have been made.

## V. CONCLUSION

When applying Fermi-Dirac statistics to the electrical properties of diamond layers doped by boron-ion implantation, the compensating donors are found to have very large values for the degeneracy weighting factor  $g_D$  ascribed to them. It is also found that the value of  $g_D$  depends on the annealing cycle employed after ion implantation. These results may be explained by assuming that these donor centers consist of small aggregates of vacancies, called vacloids, which can be considered as vacancy-lattice-type "crystallites." Using this assumption, reasonable estimates could also be made for the activation ratios and densities of acceptors and donors achieved when doping diamond layers by means of ion implantation.

## ACKNOWLEDGMENTS

The research described in this paper was carried out as part of a program on ion implantation into diamond, which was initiated by Dr. H.B. Dyer of the DeBeers Industrial Diamond Division and Professor J.P.F. Sellschop of the University of the Witwatersrand, and financed by DeBeers.

<sup>1</sup>J. F. Prins, Phys. Rev. B **38**, 5576 (1988).

<sup>2</sup>J. F. Prins, Nucl. Instrum. Methods B **35**, 484 (1988).

<sup>3</sup>J. F. Prins, T. E. Derry, and J. P. F. Sellschop, Phys. Rev. B **34**, 8870 (1986).

<sup>4</sup>For a review of the semiconducting properties of diamonds, see A. T. Collins and E. C. Lightowler, in *The Properties of Diamonds*, edited by J. E. Field (Academic, New York, 1979), p. 79.

<sup>5</sup>For a review of the optical properties of diamonds, see C. D. Clark, E. W. J. Mitchell, and B. J. Parsons, in *The Properties of Diamonds*, edited by J. E. Field (Academic, New York, 1979), p. 23.

<sup>6</sup>C. D. Clark, R. W. Ditchburn, and H. B. Dyer, Proc. R. Soc. London, Ser. A **237**, 75 (1956).

<sup>7</sup>J. F. Prins, Phys. Rev. B **31**, 2472 (1985).

<sup>8</sup>See, for example, J. S. Blakemore, *Semiconductor Statistics* (Pergamon, New York, 1962).

<sup>9</sup>J. F. Ziegler, J. P. Biersack, and U. Littmark, *The Stopping and Range of Ions in Solids* (Pergamon, New York, 1985).

<sup>10</sup>T. E. Derry, R. W. Fearick, and J. P. F. Sellschop, Nucl. Instrum. Methods **170**, 407 (1980).

<sup>11</sup>J. W. Vandersande, J. Phys. C **13**, 759 (1980).

<sup>12</sup>E. Pereira, and M. I. B. Jorge, Solid State Commun. **61**, 75 (1987).